NUCLEAR DATA AND MEASUREMENTS SERIES

ANL/NDM-46

Fast-Neutron Total and Scattering Cross Sections of ^{107}Ag in the MeV Region

by

A. Smith, P. Guenther, G. Winkler, and J. Whalen

January 1979

ARGONNE NATIONAL LABORATORY,
ARGONNE, ILLINOIS 60439, U.S.A.

NUCLEAR DATA AND MEASUREMENTS SERIES

ANL/NDM-46

FAST-NEUTRON TOTAL AND SCATTERING CROSS SECTIONS OF ^{107}Ag IN THE MeV REGION

by

A. Smith, P. Guenther, G. Winkler and J. Whalen

Argonne National Laboratory

January 1979

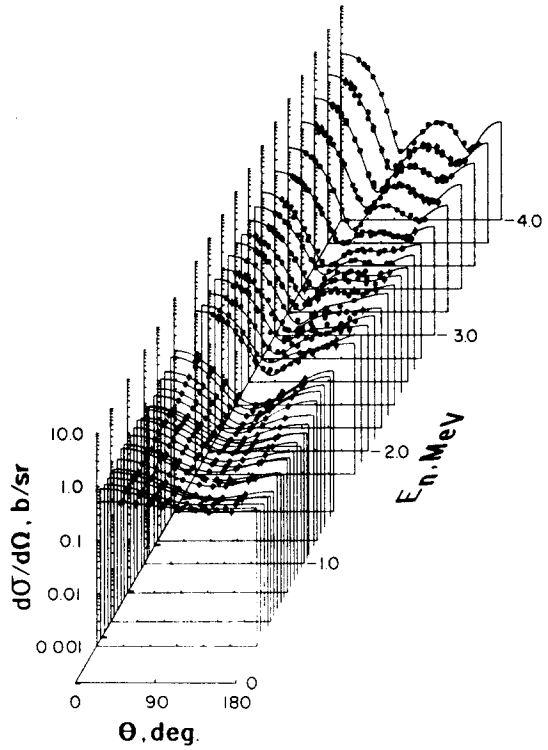

U of C-AUA-USDOE

ARGONNE NATIONAL LABORATORY,
ARGONNE, ILLINOIS 60439, U.S.A.

The facilities of Argonne National Laboratory are owned by the United States Government. Under the terms of a contract (W-31-109-Eng-38) between the U. S. Department of Energy, Argonne Universities Association and The University of Chicago, the University employs the staff and operates the Laboratory in accordance with policies and programs formulated, approved and reviewed by the Association.

MEMBERS OF ARGONNE UNIVERSITIES ASSOCIATION

The University of Arizona
Carnegie-Mellon University
Case Western Reserve University
The University of Chicago
University of Cincinnati
Illinois Institute of Technology
University of Illinois
Indiana University
Iowa State University
The University of Iowa
Kansas State University
The University of Kansas
Loyola University
Marquette University
Michigan State University
The University of Michigan
University of Minnesota
University of Missouri
Northwestern University
University of Notre Dame
The Ohio State University
Ohio University
The Pennsylvania State University
Purdue University
Saint Louis University
Southern Illinois University
The University of Texas at Austin
Washington University
Wayne State University
The University of Wisconsin

ANL/NDM-46

FAST-NEUTRON TOTAL AND SCATTERING CROSS SECTIONS OF ^{107}Ag IN THE MeV REGION

by

A. Smith, P. Guenther, G. Winkler and J. Whalen

Argonne National Laboratory

January 1979

Applied Physics Division
Argonne National Laboratory
9700 South Cass Avenue
Argonne, Illinois 60439
USA

NUCLEAR DATA AND MEASUREMENTS SERIES

The Nuclear Data and Measurements Series presents results of studies in the field of microscopic nuclear data. The primary objective is the dissemination of information in the comprehensive form required for nuclear technology applications. This Series is devoted to: a) measured microscopic nuclear parameters, b) experimental techniques and facilities employed in measurements, c) the analysis, correlation and interpretation of nuclear data, and d) the evaluation of nuclear data. Contributions to this Series are reviewed to assure technical competence and, unless otherwise stated, the contents can be formally referenced. This Series does not supplant formal journal publication but it does provide the more extensive information required for technological applications (e.g., tabulated numerical data) in a timely manner.

TABLE OF CONTENTS

	Page
ABSTRACT	1
I. INTRODUCTION	2
II. MEASUREMENT METHODS	3
III. EXPERIMENTAL RESULTS	6
IV. PHYSICAL INTERPRETATION	18
V. SUMMARY REMARKS	29
ACKNOWLEDGEMENTS	31
REFERENCES	32

FAST-NEUTRON TOTAL AND SCATTERING CROSS SECTIONS OF ^{107}Ag IN THE MeV REGION*

by

A. Smith, P. Guenther, G. Winkler[a] and J. Whalen

Argonne National Laboratory

ABSTRACT

Neutron total cross sections are measured from 0.25 to 4.5 MeV at intervals of $\lesssim$10 keV. Neutron differential elastic- and inelastic-scattering cross sections are measured from 1.5 to 4.0 MeV at intervals of $\leq$0.2 MeV. Cross sections for scattering into more than 20 energy groups are determined. Cross sections calculated from an optical-statistical model are in quantitative agreement with measured neutron total and elastic-scattering cross sections and in qualitative agreement with measured neutron inelastic-scattering cross sections. In the context of this model, significant dependence of the inelastic-scattering process on parity and/or deformation is not in evidence. The interpretation of the observed neutron inelastic-neutron-scattering results is consistent with previous reported J^{π} assignments and the systematics of nuclear-level-densities.

*This work supported by the U.S. Department of Energy.

[a]Permanent Address: Institut fuer Radiumforschung und Kernphysik, A-1090 Vienna, Boltzmanngasse 3, Austria.

I. INTRODUCTION

^{107}Ag lies in an "island" of isomerism due to the close energy coincidence of $2p_{1/2}$ and $1g_{9/2}$ shells.[1] The latter is preferentially filled with eight protons. A single proton in the $2p_{1/2}$ shell governs the ground-state spin and parity of 1/2-. 7/2+ and 9/2+ levels of the $g_{9/2}$ shell are found at low excitation energies (i.e. $\sim$100 keV). Transitions to the ground state from these positive-parity levels are via M4 radiation, relatively slow and thus exhibit the isomeric behavior. Subsequent excited levels follow positive and negative parity sequences based upon the first-excited and ground-state configurations, respectively. A duality of optical potentials has been reported from fast-neutron scattering studies in this mass region (i.e. scattering of $\sim$1.0 MeV neutrons from ^{103}Rh).[2] One potential provided a description of scattering to the odd-parity levels while another, and quite different one, was found suitable for even-parity levels. The observed phenomenon was large; amounting to a factor of two or more in the neutron inelastic-scattering cross sections. It is conceivable that the single $p_{1/2}$ proton may polarize the even core with the consequence of significant direct-reaction excitation of low-lying levels.[3] The present studies were primarily undertaken to examine the reported parity dependence of the optical potential and secondarily to ascertain, if possible, the contribution of the direct-reaction mechanism to the neutron inelastic-scattering processes. The study extended from energies where the compound-nucleus components are large and the level structure reasonably well known to energies where the neutron elastic scattering is essentially all due to a direct process and thus relatively easily interpreted in terms of an optical potential.

^{107}Ag is a fission product. A model quantitatively descriptive of neutron-induced processes in the fission-product region is of considerable

applied interest. The deduction and verification of such a model was an additional objective of the present work.

Subsequent portions of this paper: a) outline the experimental methods employed in the measurements (Sec. II), b) summarize the experimental results (Sec. III), c) discuss some physical interpretations (Sec. IV), and d) briefly summarize the work (Sec. V).

II. MEASUREMENT METHODS

A. Sample

All of the measurements employed a cylindrical sample of metallic silver 2 cm in diameter and 2 cm long.[4] The isotopic purity was 98.22 atom-percent ^{107}Ag and 1.78 atom-percent ^{109}Ag. In addition, there were some minor chemical impurities with abundances of less than a few hundred weight-parts per million. The experimental results were analyzed assuming the sample was entirely ^{107}Ag as corrections for contaminant contributions were estimated and found to be considerably less than the respective experimental uncertainties. It was assumed that the sample was of uniform density and this assumption was consistent with the results of simple tests such as weight and balance. However, it was impractical to destroy the rare sample for more detailed density assay. A non-uniform density could significantly affect only the neutron total-cross-section results.

B. Neutron-Total-Cross-Section Measurements

The neutron-total-cross sections were deduced from the observed axial transmission of pseudo-monoenergetic neutrons through the silver sample in a conventional manner.[5] The neutron source was the $^{7}Li(p,n)^{7}Be$ reaction with the incident neutron energy spread of $\sim$50 keV determined by the thickness of the lithium-source metallic film.[6] A large shield and collimator defined a neutron beam with a diameter of $\sim$1 cm at a zero-degree source-reaction

angle. The neutron detector was an organic scintillator placed on the neutron-beam axis 5-7 m from the source. The neutron source was operated in a pulsed mode with neutron bursts of $\sim$1 n sec at a repetition rate of 2 MHz. The time-of-flight of the neutrons from the source to detector was measured. The resulting neutron-velocity spectra were analyzed in such a manner as to reject the second, and minor, neutron group from the source reaction and properly account for small background effects. The silver transmission sample was placed on a wheel together with reference carbon samples. The wheel interchanged samples and voids in the neutron beam approximately 50 times per minute. Data acquisition was correlated with the sample-void positions using a digital computer. Independent monitoring of source intensity was not required. Cross sections deduced from the carbon reference sample were used to verify the fidelity of the apparatus.[7] An ancillary set of measurements employed carbon, silicon and sulfur samples. The results of the latter measurements, together with the observed threshold of the source reaction, defined the neutron energy scale relative to well known neutron-resonance energies and the Q-value of the $^{7}Li(p,n)^{7}Be$ reaction.[6,8,9] The energy scale was believed to be known to better than 10 keV, i.e. to much better accuracy than the energy resolution employed in the present silver measurements. Details of the measurement apparatus and associated techniques are given elsewhere.[10]

C. Neutron-Scattering Measurements

The neutron-scattering measurements were made using the pulsed-beam time-of-flight technique and the 10-angle detection apparatus at the Argonne Fast Neutron Generator.[11] The $^{7}Li(p,n)^{7}Be$ reaction was again used as a neutron source with the metallic lithium film arranged to provide incident-neutron energy spreads at the scattering samples of 10-50 keV.[6] The neutron source intensity was monitored using a special-purpose time-of-flight system employing a small plastic scintillator and with several "long counters."

Ten neutron detectors were arranged between scattering angles of $\sim$20-160°. The angular positions of the detectors were variable and two or more angular settings were generally used at a given incident energy resulting in twenty or more angle-differential measurements per scattered neutron group. The angular settings of the detectors were optically determined to within <0.5°. The absolute normalization of the angular system was established to within <1.0° by observation of neutrons scattered from hydrogen at a given incident energy both left and right of the source-reaction center line. The angular setting was further verified by observation of the well known minimum in the carbon-differential-elastic-scattering cross sections near 3.5 MeV.[7] The scattered-neutron flight paths were generally $\sim$5 m. A few selected measurements were made at scattered-neutron flight paths of $\sim$20 m in order to obtain optimum velocity resolutions. Relative energy-dependent detector sensitivities were determined by the observation of neutrons scattered from hydrogen at a fixed incident energy and a variety of angles and/or by the observation of neutrons emitted at the spontaneous fission of ^{252}Cf.[12,13] The normalization of the relative detector sensitivities was established by observation of neutrons scattered from hydrogen at each incident measurement energy.[12] Thus all ^{107}Ag scattering cross sections were determined relative to the well known H(n,n) cross sections.[14] The ten detector-velocity spectra and that of the monitor were stored within a digital computer system. Subsequent off-line data processing integrated neutron groups identified in the measured velocity spectra and reduced the integrated-spectra responses to differential-scattering cross sections. These results were corrected for

multiple-event, beam attenuation and angular resolution effects associated with both the primary ^{107}Ag measurements and the reference H(n,n) scattering standard.[15] Concurrently, the differential elastic scattering cross sections o carbon were routinely determined in order to verify the instrument performance.

The above measurement techniques and the particular apparatus have been extensively described on previous occasions. More detailed information is available in references 13 and 15.

III. EXPERIMENTAL RESULTS[a]

A. Neutron Total Cross Sections

The primary experimental objective was the measurement of the energy-averaged neutron total cross section comparable with the differential scattering results (below) and with the predictions of energy-averaged physical models (e.g. optical-statistical and coupled-channels models). Thus good cross section accuracies were sought with broad incident-energy resolutions. The cross-section measurements were made from $\tilde{\sim}$0.25 to 4.5 MeV in steps of $\lesssim$10 keV with incident energy resolutions of 30-50 keV. The measurements were made during several widely separated measurement periods with consistent results. The individual experimental values were averaged over energy intervals of 20-50 keV to obtain the final total cross-section results shown in Fig. 1. Generally, the neutron-total-cross-section results smoothly decreased with energy with no clear indication of intermediate structure as illustrated. The statistical accuracies of the averaged data points were $\lesssim$2%. Known systematic uncertainties were generally believed much smaller.

---

[a] All numerical experimental values resulting from this work have been transmitted to the National Nuclear Data Center, Brookhaven National Laboratory.

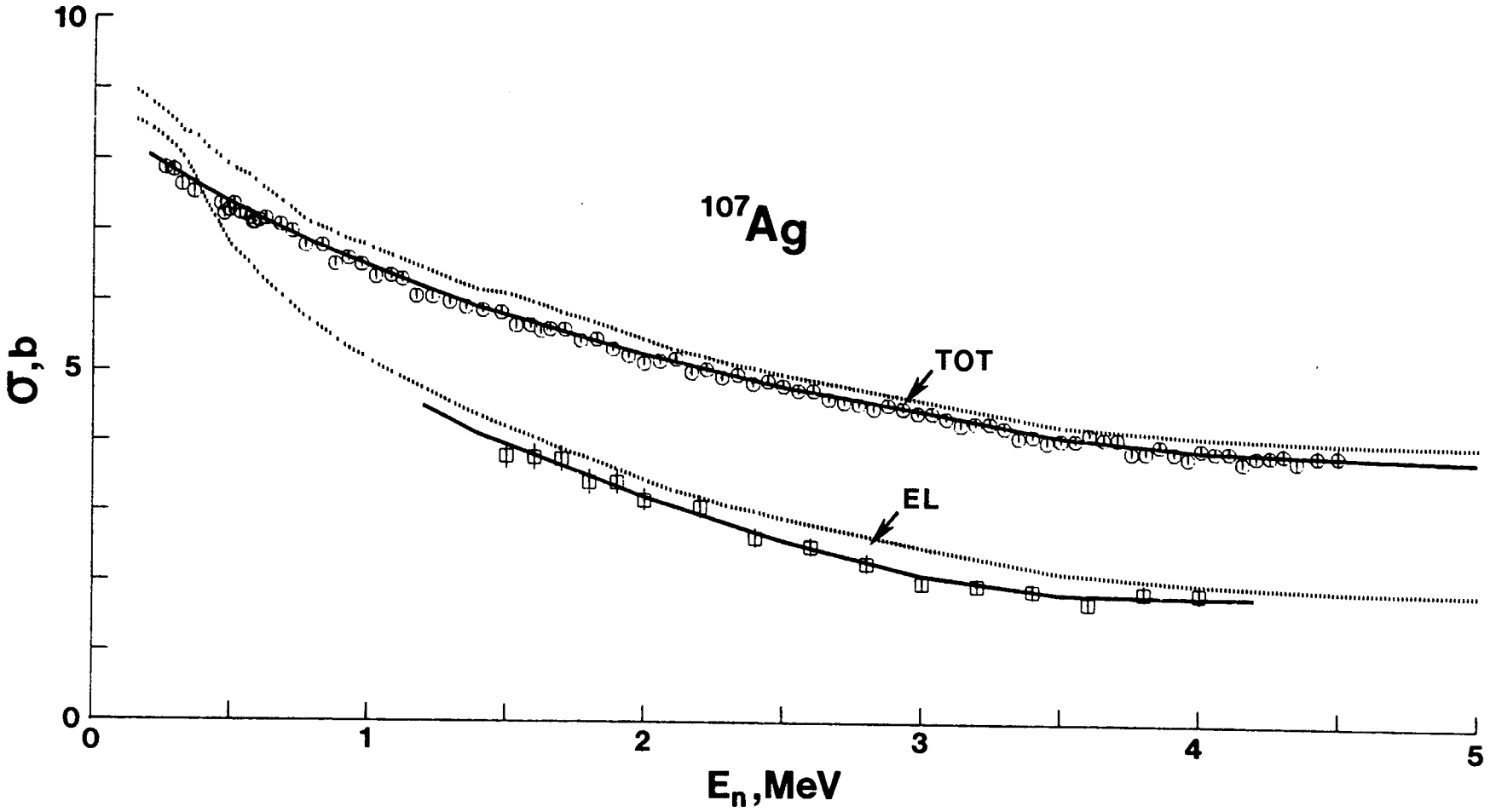

Fig. 1. ^{107}Ag Measured Neutron Total (circular data points) and Angle-integrated Elastic-scattering (square data points) Cross Sections. Solid curves are "eyeguides" constructed through the present measured values. The dotted curves denote the comparable ENDF/B-IV values.

A possible exception was the uncertainty associated with the uniformity of the sample density. This was believed negligibly small but was not verified, as outlined above.

Apparently, no comparable experimental neutron-total-cross-section results have been reported in the literature. The present results are 2-6% lower than reported elemental values.[16] They are similarly lower than the neutron total cross sections of ^{107}Ag given in ENDF/B-IV[17] as illustrated in Fig. 1. This is not surprising as the evaluation, in the absence of measured isotopic values, appears to be based upon the elemental results.

B. Neutron Elastic Scattering Cross Sections

The differential neutron elastic-scattering cross sections were measured at incident neutron energy intervals of 100 keV from 1.5 to 2.0 MeV and at 200 keV intervals from 2.0 to 4.0 MeV and over the scattered-neutron angular range 20°-160°. The incident-neutron energy spreads were $\sim$20-30 keV. The experimental scattered-neutron velocity resolution with flight paths of $\sim$5 m was sufficient to resolve the elastically-scattered neutron component from all known inelastic-neutron groups to incident energies of $\sim$3.0 MeV. The resolutions were less favorable at energies above 3.0 MeV. However, selected measurements with better resolution obtained with a 20 m flight path indicated that inelastically scattered neutrons did not appreciably contaminate the "elastic" neutron groups observed at the shorter (5 m) flight path The majority of the differential measurements made during three widely separate periods were consistent and thus were combined to obtain the final data set outlined in Fig. 2.

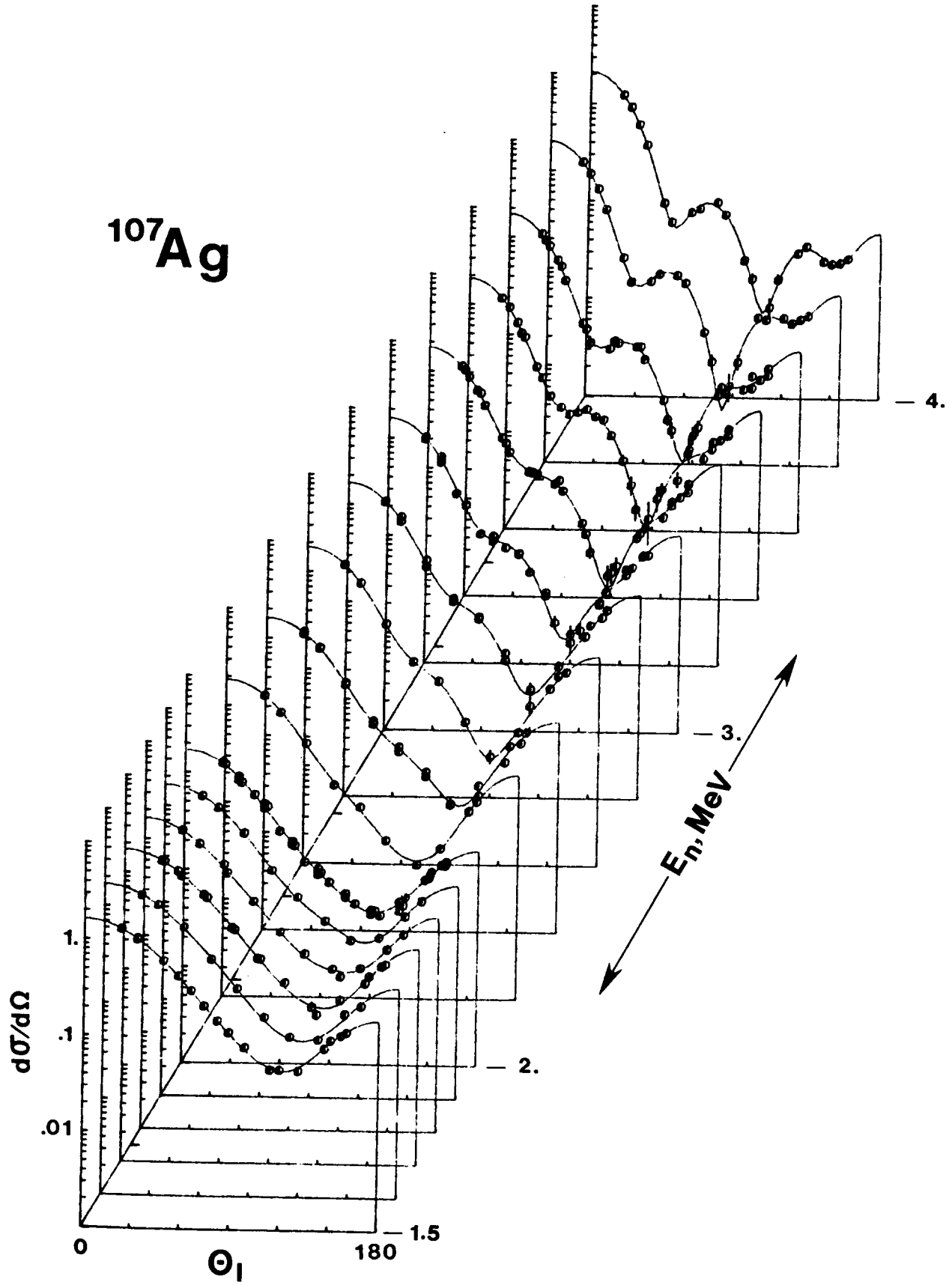

Fig. 2. Measured Differential Neutron Elastic Scattering Cross Sections of ^{107}Ag (data points). Curves indicate the results of least-square fits of Legendre polynomial series to the measured values as outlined in the text.

The statistical uncertainties of the individual differential cross sections were generally small ($\lesssim$2%) except near the deep minima. Uncertainties associated with the determination of detector efficiencies were estimated to be $\sim$3%. The measured efficiencies were reproducible to that accuracy and were supported by concurrent measurements of the differential elastic-scattering cross sections of carbon. Uncertainties due to correction procedures were generally $\lesssim$2%; again excepting regions near the deep minima. Thus the overall uncertainties in the differential elastic-scattering values were generally $\sim$5%. Results obtained at the different measurement periods were consistent to well within this estimate.

The angle-integrated elastic-scattering cross sections were deduced from the measured differential values by least-square fitting a six-order Legendre polynomial series to each experimental distribution. These series were descriptive of the measured values as illustrated in Fig. 2. The corresponding angle-integrated cross sections are shown in Fig. 1. The overall uncertainties in the angle-integrated values were estimated to be $\sim$5%. The elastic-scattering cross sections and the above neutron total cross sections imply non-elastic-scattering cross sections with an accuracy of 5-7%. This non-elastic result is generally consistent with the inelastic-neutron scattering results discussed below.

There are apparently no previously reported experimental results with which to compare the present elastic-scattering values. However, the present elastic-scattering results are qualitatively similar to those previously observed at this laboratory in the same general mass-energy region (i.e. the even isotopes of zirconium and molybdenum).[13,18] The present angle-integrated elastic scattering cross sections are generally $\sim$10% smaller than the comparable values given in ENDF/B-IV.[17] The latter appear to be the result of model calculations.

C. Neutron Inelastic-Scattering Cross Sections

Neutron inelastic-scattering cross sections were determined concurrently with the above elastic-scattering measurements. Most of the measurements were made at scattered-neutron flight paths of 5 m, with improved resolution measurements at 2.5 and 3.0 MeV using 20 m flight paths. Scattering angles were in the range 20-160°. Incident-neutron resolutions varied from 10-30 keV. The scattered-neutron resolutions varied widely depending upon the particular experimental configuration and the incident and exit neutron energies. Generally a cross section determination was made when at least five differential-cross-section values were available at a given incident-neutron energy. The angle-integrated cross sections were determined from the fitting of a Legendre polynomial series to the differential values in a manner analogous to that outlined above in the context of elastic scattering. Most of the observed inelastic-neutron distributions were nearly isotropic as illustrated in Fig. 3. Thus the order of the polynomial used in the fitting procedure was low (e.g. through the P_2 term). A number of the measurements suggested that the observed neutron groups were composites of two or more components. This was particularly true of neutron groups corresponding to excitations of more than 1.0 MeV and was consistent with the complex level structure recently observed by Reitmann et al.[19] in $(n;n',\gamma)$ measurements. Some of the observed inelastically-scattered neutron groups were perturbed by contributions from the small-intensity second neutron group from the neutron-source reaction, $^{7}Li(p,n)^{7}Be$. In these cases corrections were made using the intensity ratios given in Ref. 20.

The observed inelastic-neutron excitation energies were determined from measured flight paths, flight times and incident-neutron energies and verified by the observation of neutron groups resulting from well known inelastic scattering processes (e.g. scattering from ^{56}Fe). The resulting excitation

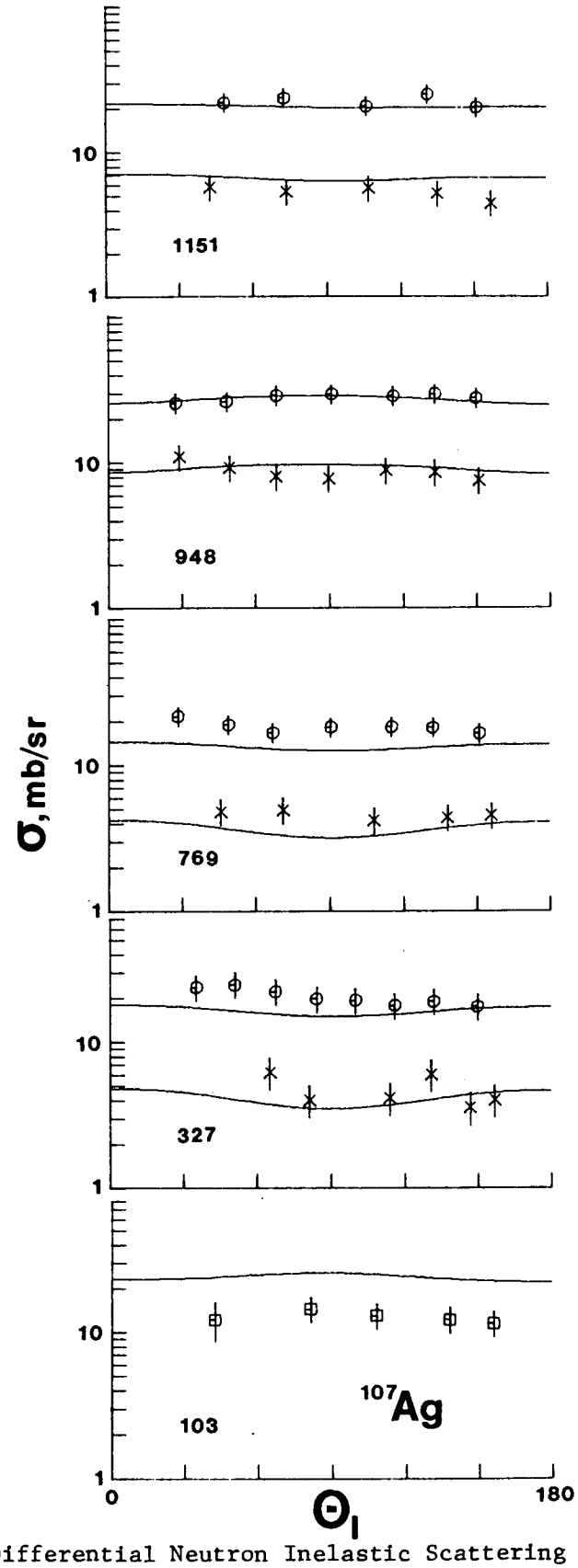

Fig. 3. Illustrative Differential Neutron Inelastic Scattering Cross Sections of ^{107}Ag. Excitations are numerically defined in keV. Measured values are noted by data points with □ = 1.5 MeV incident energy, X = 2.0 MeV and ○ = 3.0 MeV. Scattering angles are in degrees-lab, cross sections in mb/sr. Curves indicate the results of model calculations as discussed in Sec. IV of the text.

energies are summarized in Table 1. The stated uncertainties are relevant to the mean observed values and defined as the RMS deviation from the mean of at least five measurements. In some cases there were more than 30 independent measurements of the excitation energy. These uncertainties should not be confused with the scattered-neutron resolutions as the latter were not only determined by the experimental arrangement but also by the complexity of the underlying physical structure. Throughout, the objective was the correlation of the present experimental results with reported level structure. Precise energies can be better determined using alternate techniques (e.g. studies of the $(n;n',\gamma)$ process using a GeLi detector).

More than 20 scattered neutron groups were observed. They were correlated with previously reported level structure as given in Refs. 19 and 21. The first group was attributed to the reported 93(7/2+)-126(9/2+) keV doublet. The cross sections are relatively small and the levels closely spaced thus the two components were not clearly resolved in the present measurements. The experiments did not resolve the third group from the elastic-scattering component due to the second neutron group from the source reaction. Thus the excitation energy was only qualitatively determined and the corresponding cross sections subject to large corrections resulting in increased uncertainties. The observed 769 keV group was attributed to the reported 787(3/2-) level. At least three levels have been reported in the vicinity of 950 keV (922(5/2+), 949(5/2-) and 973(?) keV). The fifth observed group at 948 keV was attributed to the collective sum of contributions from all three reported levels. A marginally observed group corresponding to a level at 1054 keV probably corresponds to the reported level at 1049 keV. The seventh observed group corresponds to an excitation of 1151 keV. It probably is the result of contributions from the three reported levels at 1049, 1094 and 1143 keV. All higher excitations observed in the present experiments are

TABLE 1. Observed ^{107}Ag Excitation Energies[a]

No.	E_x (keV)	No.	E_x (keV)
1	103 ± 16	14	1870 ± 15
2	327 ± 22	15	1942 ± 17
3	425[b]	16	2039 ± 31
4	769 ± 23	17	2164 ± 30
5	948 ± 29	18	(2270)
6	(1054)	19	(2314)
7	1151 ± 21	20	(2389)
8	1242 ± 27	21	(2436)
9	1326 ± 19	22	(2494)
10	1386 ± 25	23	(2555)
11	1487 ± 20	24	(2620)
12	(1595)		
13	(1659)	1632 ± 25	

[a]Uncertainties are RMS deviations from the mean of at least five measurements. Uncertain values are in parenthesis. Brackets indicate groups that were combined in the respective cross section determinations.

[b]Value is uncertain by $\tilde{\sim}$50 keV due to perturbations from the second neutron group of the source reaction (see text).

almost certainly composites of contributions from two or more levels. This assumption is reasonably consistent with the reported density of levels to excitations of 1.7 MeV as given in Ref. 19. Above 1.7 MeV the level density increases very rapidly and far exceeds the experimental ability to resolve individual components.[22]

The measured angle-integrated neutron-inelastic-scattering cross sections are summarized in Fig. 4A and B to excitations of $\tilde{\sim}$2.0 MeV. The illustrated uncertainties are the results of subjective judgements governed primarily by experimental resolutions but also including considerations of counting statistics, detector efficiencies and correction procedures. Cross sections corresponding to excitations greater than $\tilde{\sim}$2.0 MeV were generally obtained at only a very few incident energies and thus the excitation functions were not well defined. "Eye-guides" were constructed (aided by the calculations outlined below) through the measured values as illustrated in Fig. 4A and 4B. These "eye-guides" were then summed to obtain the total-neutron-inelastic-scattering cross section. The resulting sum was consistent to within several percent with the non-elastic-scattering cross section deduced from the above measured neutron total and elastic-scattering cross sections.

A few experimental studies of inelastic neutron scattering from elemental silver have been reported in the literature (e.g. see CINDA 76/77).[23] These previous results are not easily compared with the present measured values as the two isotopes of the element (107 and 109) have similar and complex excited structure. There appear to have been no previously published experimental studies of inelastic-neutron scattering from the isotope ^{107}Ag in an energy range comparable with the present results.

Fig. 4A

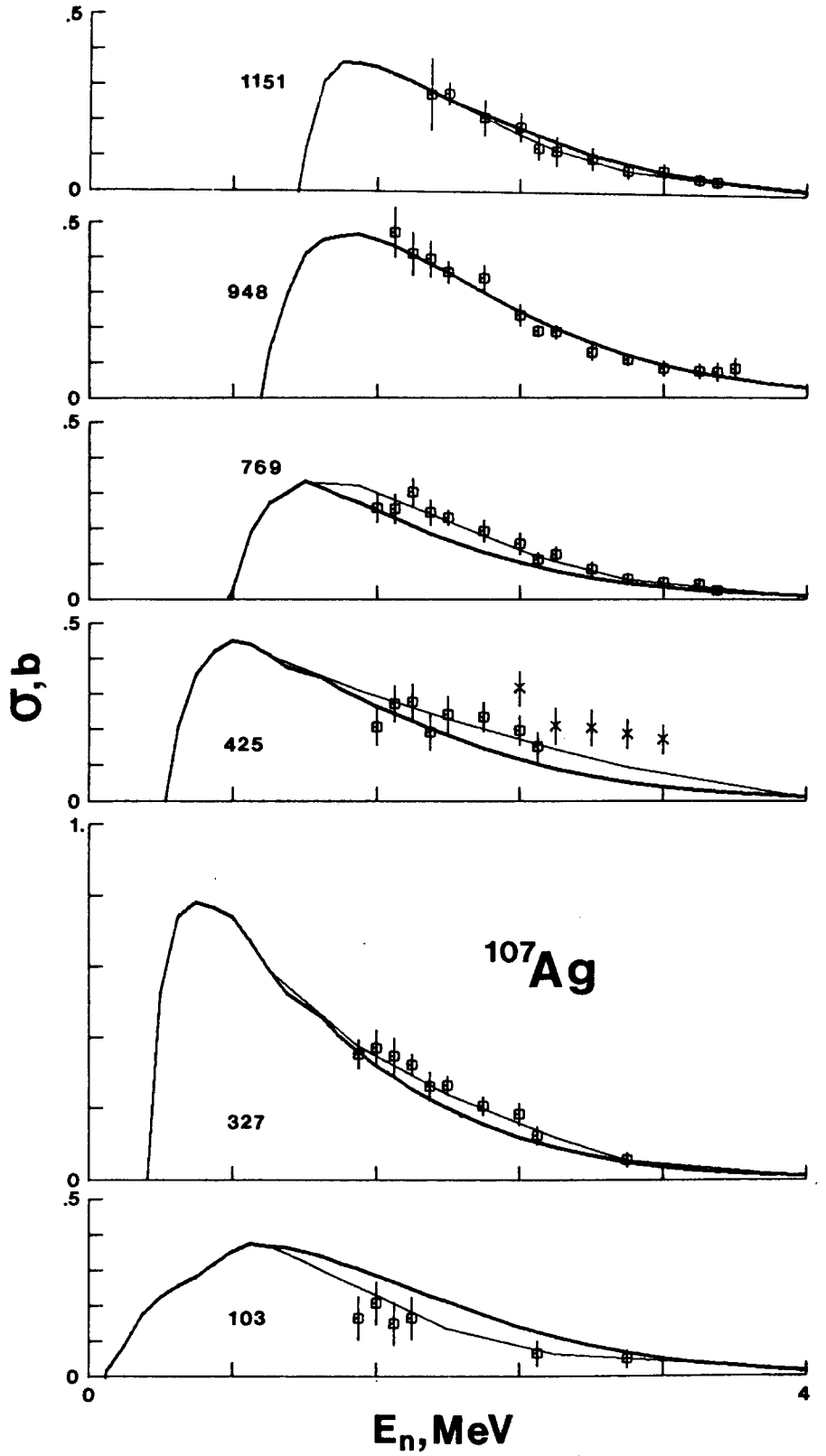

Fig. 4A & B. Inelastic Neutron Excitation Cross Sections of ^{107}Ag. Numerical excitation energies are given in keV. Square symbols indicate measured values. Cross symbols refer to measurements combining the cross sections for the indicated excitation with those of the preceding (and lower energy) excitation. The heavy curves indicate the results of model calculations as described in Sec. IV of the text and the light curves are "eyeguides" constructed through the measured and/or calculated values.

Fig. 4B

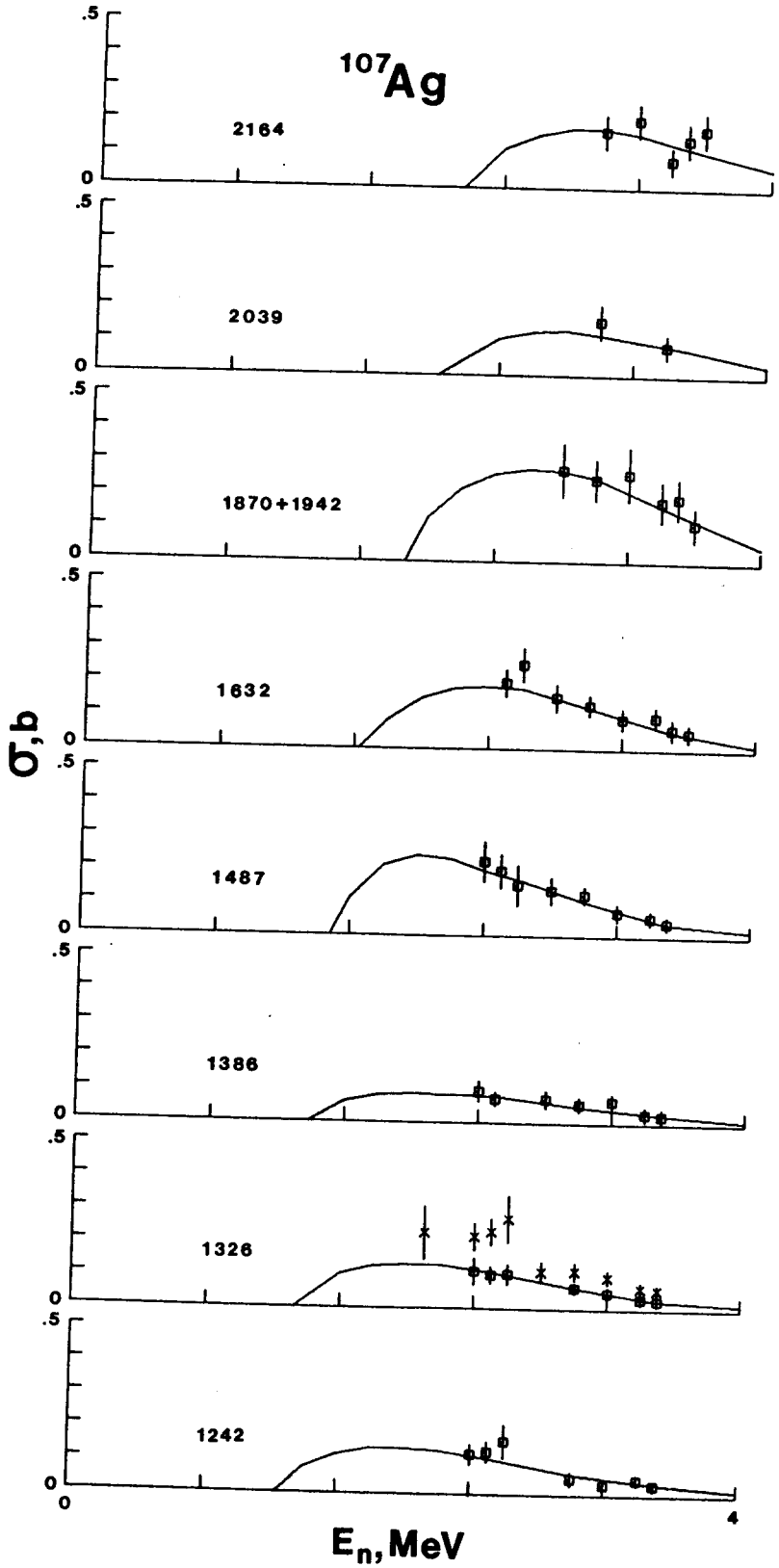
^{107}Ag
2164
2039
1870+1942
1632
1487
1386
1326
1242
.5
0
σ,b
4
E_n,MeV

IV. PHYSICAL INTERPRETATION

The interpretive procedure was the derivation of a representative optical potential from the measured neutron total and elastic-scattering cross sections followed by the subsequent application of that potential and associated statistical concepts in the assessment of compound-nucleus (primarily neutron inelastic-scattering) cross sections.

A. A Spherical Optical Potential

The observed neutron elastic-scattering and total cross sections were utilized to deduce a spherical optical potential consisting of a Saxon real term, a Saxon-derivative absorption term and a real spin-orbit term of the Thomas form.[24] Compound-nucleus contributions were calculated using the Hauser-Feshbach formula[25] with width-fluctuation corrections having two degrees of freedom.[26] The calculations were carried out using the computer codes ABAREX-1 and -2.[27] Both programs have the capability of concurrently least-square fitting measured neutron differential-scattering and total cross sections.

The potential was primarily deduced from 6-parameter fitting (real and imaginary strengths, radii and diffusenesses) to the measured differential elastic-scattering cross sections. Neutron total cross sections were introduced into the fitting procedure with a relatively low weight (e.g. equal to that of a single differential value). The fitting procedures were confined to two incident-energy regions. In the first (1.5 to 2.0 MeV) it was assumed that the compound-elastic contribution was large and calculable. The neutron elastic-scattering calculations assumed $\tilde{\sim}20$ excited states taken from Refs. 21 and 19. Where J^{π} values were not known from previous work, assignments were made based upon statistical distributions. The 1.5 and 2.0 MeV elastic distributions were given most consideration as

they were detailed and were derived from redundant measurements. In the second energy region (3.4 to 4.0 MeV) it was assumed that compound-elastic scattering was negligibly small and thus the observed distributions could be described by shape-elastic scattering alone. The fitting procedures were carried out at each measured energy in both of the above energy intervals. The resulting parameters varied somewhat from energy-to-energy reflecting experimental uncertainties and possibly, at the lower energies, actual physical fluctuations in the data. The real-potential strength decreased with energy in a manner consistent with the form $V = V_0 - 0.3 \cdot E_n$ (MeV)[28] and this energy dependence was accepted for subsequent calculations. No clear energy-dependent trend of the absorption strength could be identified from the analysis of the present experiments. The parameters derived from the individual fitting procedures were averaged to obtain the general parameter set given in Table 2. This parameter set is similar to other sets found applicable in this mass-energy region.[18]

The above procedures were not appropriate to the intermediate energy region (i.e. >2.0 MeV and <3.5 MeV) where the compound-elastic scattering remains appreciable but knowledge of the contributing structure is far too deficient for quantitative calculation of compound-nucleus contributions. Therefore elastic scattering in the region 2.2 to 3.4 MeV was calculated by adding an adjusted compound-elastic component to the shape-elastic contribution so as to optimize the description of the measured values while, at the same time, maintaining a smooth energy dependence of the compound-elastic contribution. The resulting compound-elastic-scattering cross sections behaved in a reasonable manner, generally decreasing with energy, as illustrated in Fig. 5.

TABLE 2. Optical-Model Parameters

V_0^a (MeV) (real strength)	49.74	W^c (MeV) (imaginary strength)	7.35
R_v^b (F) (real radius)	1.211	R_w^b (F) (imaginary radius)	1.190
A_v (F) (real diffuseness)	0.604	A_w (F) (imaginary diffuseness)	0.707

[a]Saxon form assuming linear energy dependence, i.e. $V = V_0 - 0.3 \cdot E$ (MeV).

[b]Radius = $R_i \cdot A^{1/3}$.

[c]Saxon-derivative form.

In addition, a spin-orbit term of the Thomas form with an 8 MeV strength was used.

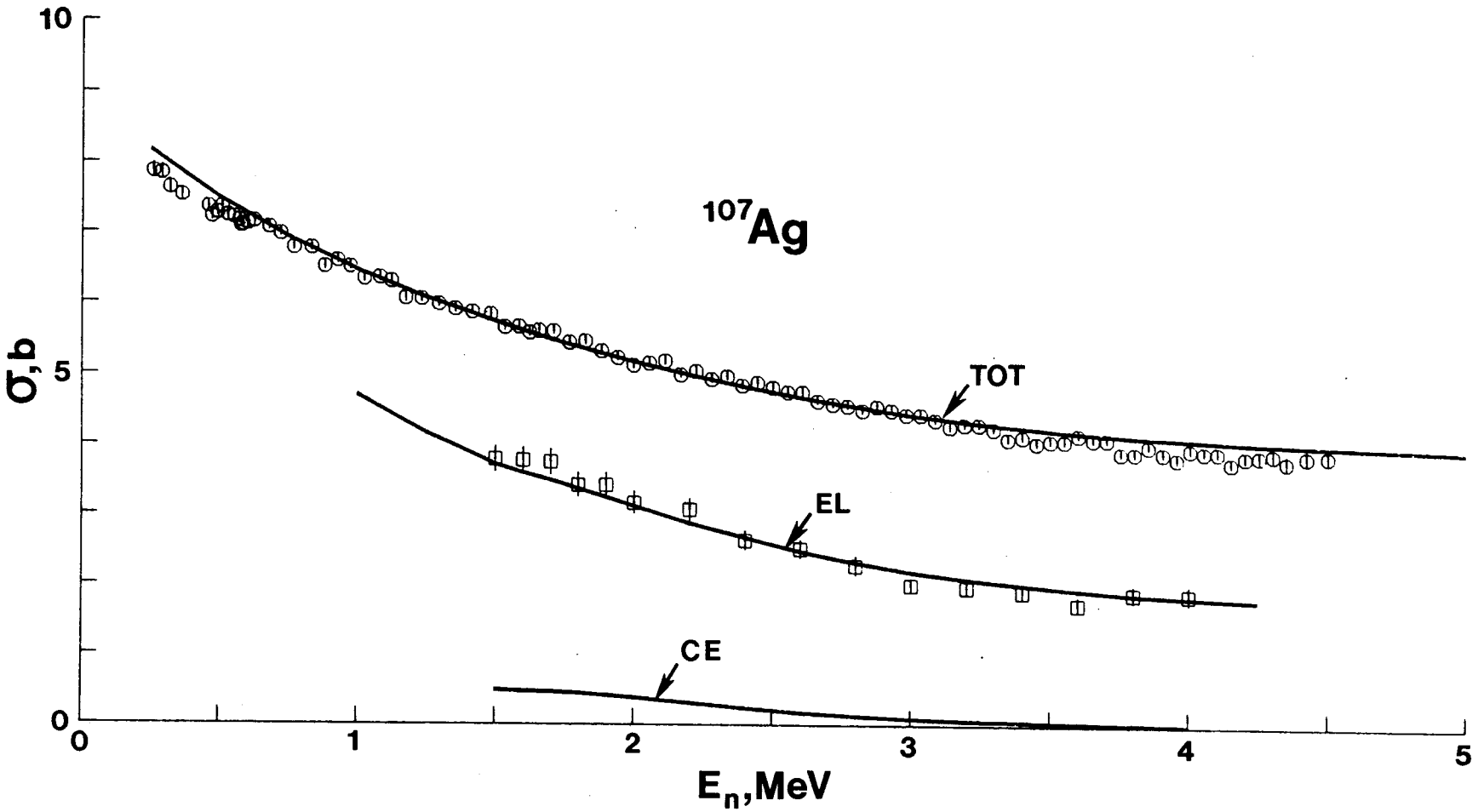

Fig. 5. Measured Neutron Total (TOT) and Angle-integrated-elastic-scattering (EL) Cross Sections of ^{107}Ag (data points) Compared with the Results of Calculations (curves). The calculated compound-elastic (CE) cross section is also indicated.

Following the above procedures an acceptable description of measured neutron total and elastic-scattering cross sections was achieved. The calculated total cross sections agree with the experimental values to within a few percent throughout the measured energy range as illustrated in Fig. 5. The largest differences are 2-3% at the extremities of the measured energy range with much better agreement over the large majority of the energy range. At the low-energy extremity the small differences between measured and calculated values may also reflect true physical fluctuations. The calculated angle-integrated elastic scattering cross sections are reasonably consistent with the values derived from the measurements, as again illustrated in Fig. 5. More than 60% of the experimentally-based results agree with those obtained by calculation to within the experimental uncertainties and the remaining values differ from those calculated by less than twice the experimental uncertainty.

The calculated differential-elastic-scattering cross sections are generally compared with the measured values in Fig. 6 and some detailed comparisons are shown in Fig. 7. In these two figures (and throughout this paper) it must be clearly understood that the calculated results were obtained with the general potential of Table 2 and are <u>not</u> the results of explicit fits to individual elastic-scattering distributions. A very large majority of the measured values are consistent with those calculated to well within the experimental uncertainties alone. A few measured values deviate from those calculated by larger amounts as should be expected from the statistical nature of the measurement process. In addition there appear to be some small systematic differences, notably at the lowest measurement energies (where the calculations tend to be a few percent low between $\sim$40-60°) and at the very highest energies and the largest scattering angles. The low-energy comparisons may be perturbed by true physical fluctuations such as those known

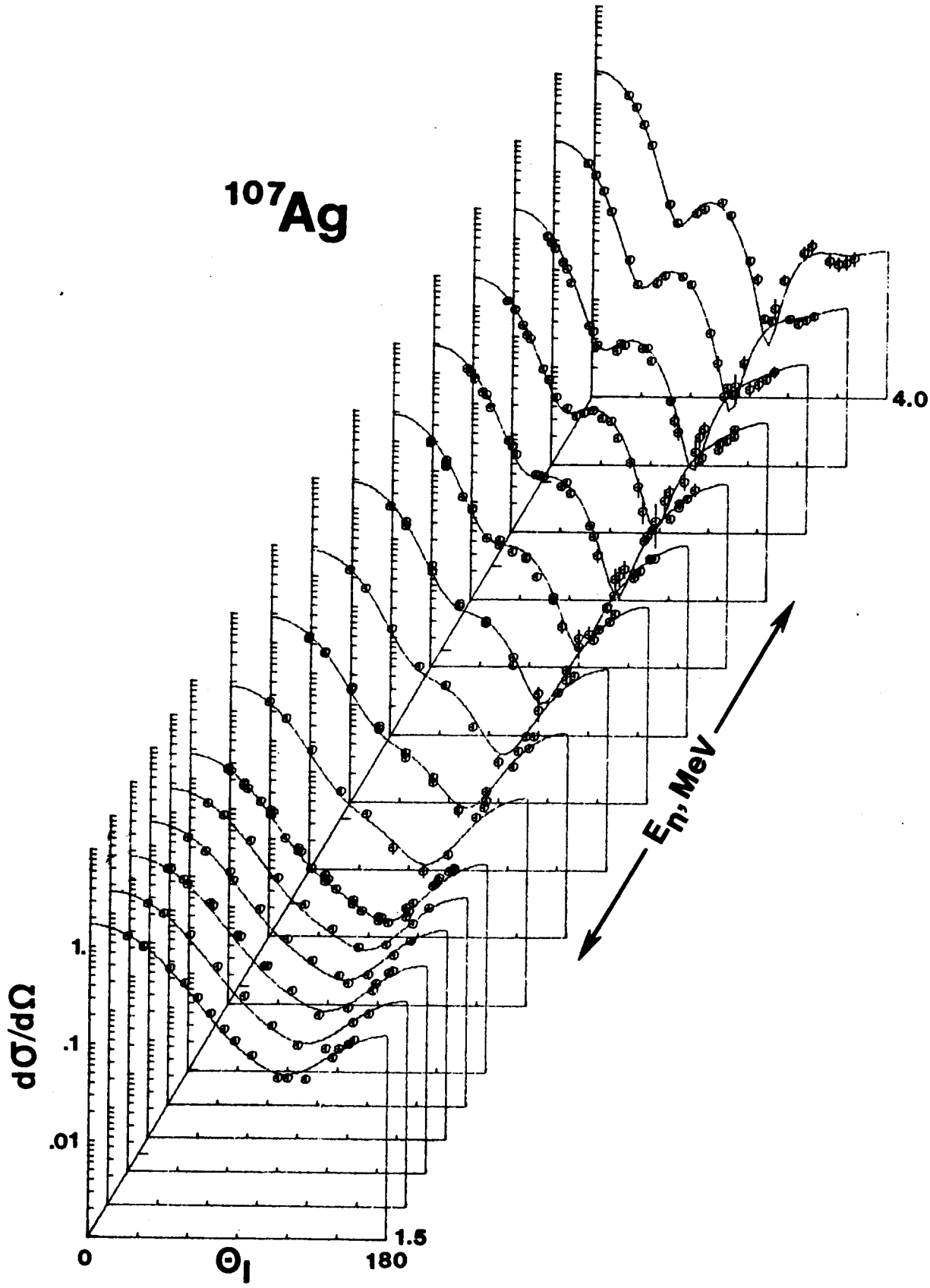

Fig. 6. Comparison of Measured (data points) and Calculated (curves) Neutron-differential-elastic-scattering Cross Sections of ^{107}Ag. Scattering angles are given in lab-degrees and differential cross sections in b/sr.

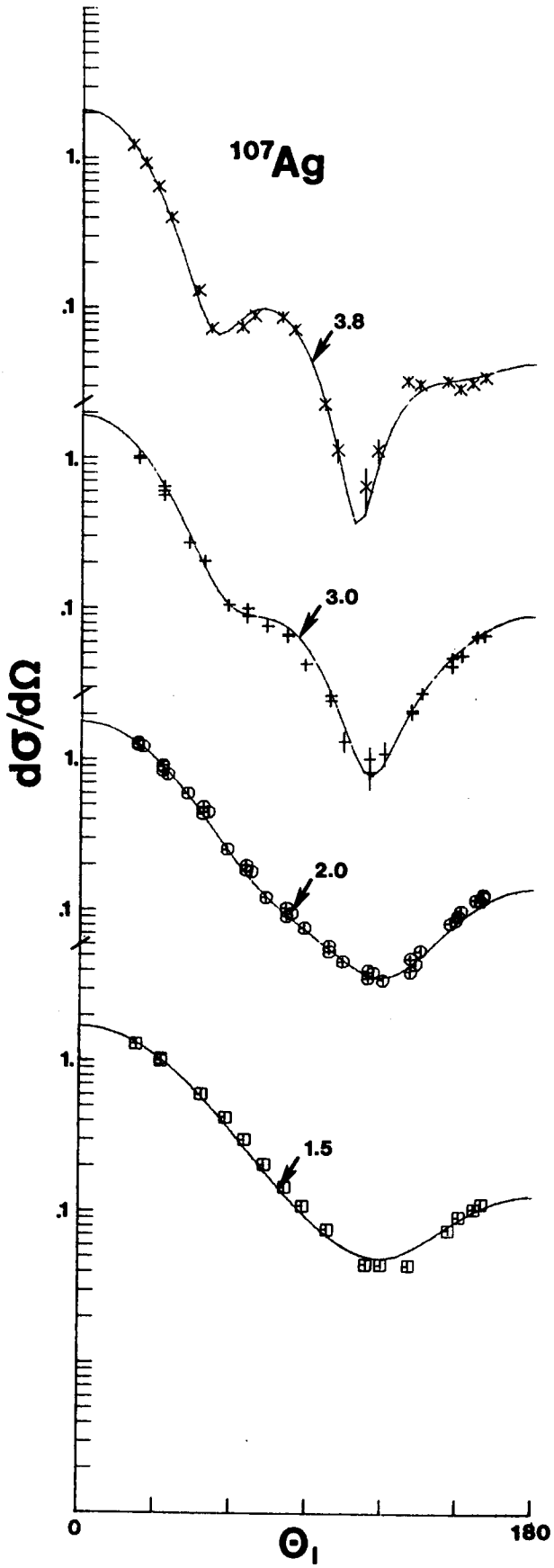

Fig. 7. Specific Comparisons of Measured (data points) and Calculated (curves) Differential-elastic-scattering Cross Sections of ^{107}Ag. Incident energies are noted in MeV, scattering-angles are in lab-degrees and cross sections are given in b/sr.

to exist in scattering from even nuclei in this mass region[18] and even in much heavier nuclei at energies of $\tilde{\sim}$1.5 MeV.[29]

While there remain some physical and experimental uncertainties in the above derivation the resulting spherical potential of Table 2 provides a reasonable basis for subsequent interpretations of inelastic neutron scattering and other aspects of the interaction of fast neutrons with ^{107}Ag.

B. Statistical-reaction Processes

The interpretation of statistical-reaction processes was based upon the above optical potential and calculational methodology. The interpretation was complicated by the uncertain knowledge of the level structure over the energy range of the present measurements. Low-lying levels (to excitation of $\tilde{\sim}$1.1 MeV) are fairly well established and were explicitly treated in the calculations. Contributions from higher-lying levels (excitations above $\tilde{\sim}$1.1 MeV) were approximated by means of the level-density formalism of Gilbert and Cameron.[22] The level-density parameters (i.e. temperature, zero-energy and spin-cutoff factor) were taken from the Gilbert and Cameron tabulation. The spins and parities of the explicitly defined levels employed in inelastic-scattering calculations were generally taken from Refs. 19 and 21 and correlated with the experimentally observed excitation energies as defined in Table 3. Calculated angle-integrated neutron inelastic scattering cross sections are compared with the corresponding experimental values in Fig. 4A and some illustrative comparisons of measured and calculated differential-inelastic-scattering cross sections are shown in Fig. 3. Generally, the agreement between measured and calculated quantities is as good as is conventionally achieved in simpler cases where the level structure is fully defined. However, there are detailed differences between measured and calculated values as discussed below.

TABLE 3. Excitation Energies Employed in the Inelastic-Neutron-Scattering Calculations[a]

No.	E_x (keV)	J^π	Exp. E_x (keV)
1	0	1/2-	0
2	93	7/2+	103
3	126	9/2+	
4	325	3/2-	327
5	423	5/2-	425
6	787	3/2-	769
7	922	5/2+	948
8	949	5/2-	
9	973	7/2-	
10	1049	1/2+	1151
11	1094	3/2+	
12	1143	5/2+	

[a]High-energy levels were treated as a statistical distribution following the level-density formulation of Gilbert and Cameron.[22]

Compound-elastic scattering calculated with the inclusion of the level-density distribution was essentially identical to that deduced above at either extreme of the measured energy range (i.e. at 1.5 and 4.0 MeV). This was not surprising as the continuum has relatively little effect at 1.5 MeV and at 4.0 MeV the compound-elastic scattering component is essentially negligible. In the intermediate energy region calculations inclusive of the continuum component result in smaller compound-elastic contributions than deduced above. The difference was largest at $\tilde{\sim}$2.0 MeV. Even at that energy the difference was approximately equivalent to the experimental uncertainties in the differential elastic-scattering cross sections or smaller. Thus the inclusion of the continuum component in the above derivation of the optical potential would introduce additional complexity with little, if any, effect on the parameter choice. It is reasonable to expect variations from the level-density model, particularly at the low energies of the present experiments. Such variations can have a relatively large effect on the inelastic-scattering channels. In the present case the calculated low-energy inelastic scattering cross sections may tend to be too large as the total compound-nucleus cross section remains fixed while there are indications that the calculated compound-elastic-scattering cross sections tend to be somewhat too small.

The excitation of the observed 103 keV level was attributed to contributions from 93(7/2+) and 126(9/2+) states. With this assumption the calculated cross sections were systematically larger than the measured values by more than the estimated experimental uncertainties. The difference may reflect the presence of competing channels not accounted for in the calculations either as discrete levels or as a continuum distribution. This

premise is consistent with the above discussion of the compound-elastic component. The experimental values may be systematically too low for the cross sections are small and difficult to experimentally resolve. In any event, the discrepancy between measurement and calculation is not more than 30% with the calculated values tending to be the larger. The observed differential cross sections are nearly isotropic and the angle-integrated values fall rapidly with energy, both characteristics of an essentially statistical process.

The observed levels at 327, 425 and 769 keV were attributed to reported states at 325(3/2-), 423(5/2) and 786(3/2-) keV, respectively. In each case the calculated cross sections tended to be somewhat smaller than the measured values (e.g. by 10-20%). The differences could be easily attributed to channel competition not fully accounted for by the general continuum of levels. In each of these three cases the differential cross sections were essentially isotropic and rapidly decreased with energy to values of only a few mb/sr at energies of 3-4 MeV.

The observed 948 keV level was attributed to the sum of contributions from reported 922(5/2+), 949(5/2-) and 973 keV levels. The spin of the latter has not been previously assigned. Calculations were carried out with accepted 5/2+ and 5/2- J-π values and with a variety of choices for the third component. A spin of 7/2 gave good agreement with the measured cross sections as illustrated in Fig. 4A. The observed 1151 keV level was attributed to the sum of reported levels at 1049, 1094 and 1143 keV. No J-π values have apparently been reported so, again, the results of calculations employing a variety of spin combinations were compared with the measured cross sections. A 1/2, 3/2 and 5/2 spin sequence led to results in good agreement with the measured cross sections. A preponderance of appreciably larger or smaller

spin values proved less satisfactory: However, the experimental comparisons do not define the order of the spin sequence or the exact values of the components. Again, the measured differential cross sections for both 948 and 1151 keV levels were essentially isotropic and rapidly decreased with energy.

No attempt was made to calculate cross sections for the excitation of levels beyond 1151 keV as the underlying structure is very complex and uncertain.

The level-density parameters of Gilbert and Cameron were used throughout the above calculations extending upward in energy from the last discrete level at $\tilde{\sim}$1.0 MeV.[22] The sensitivity of the calculational results to these parameter choices was examined. Reasonable changes in the spin-cutoff factor had a relatively minor effect on the results. The nuclear temperature was a sensitive parameter but wide variations did not improve upon the overall results obtained with the Gilbert and Cameron value of 0.590 MeV. However, the exercise did suggest that discrete neutron inelastic-scattering excitation cross sections measured well into the continuum region can be used to determine nuclear temperatures in the low-energy region not easily studied using more conventional evaporation-spectrum measurement techniques.

V. SUMMARY REMARKS

Detailed measurements of the neutron total and elastic-scattering cross sections of ^{107}Ag provided a foundation for the derivation of an optical potential. The resulting potential, similar to others found suitable in the same mass-energy region, was employed to calculate cross sections in quantitative agreement with the measured neutron total and elastic-scattering cross sections. The optical potential and associated statistical concepts,

including a level-density representation of the level continuum, were employed to calculate neutron inelastic scattering cross sections to excitations of $\tilde{\sim}$1.2 MeV. The calculated neutron inelastic-scattering cross sections were in qualitative agreement with the measured values. In particular, cross section results calculated with the present model did not display a strong parity-dependent discrepancy with measured values as suggested from studies of a similar nucleu (^{103}Rh) at somewhat lower incident neutron energies (e.g. $\lesssim$1.5 MeV).[2] The calculated results were sensitive to the choice of the nuclear-temperature parameters and it is suggested that the measurement and analysis of a few discrete-neutron-inelastic-excitation functions well into the low-energy continuum has the potential for nuclear-temperature determinations in a region not easily carried out using conventional evaporation-spectrum measurement techniques. The measured differential neutron inelastic scattering cross sections did not display an angle or energy dependence suggestive of a significant direct-reaction contribution to the inelastic scattering processes. Comparison of measured and calculated neutron inelastic scattering processes did suggest some guidelines for the assignment of heretofore unspecified spins at excitations of $\tilde{\sim}$1.0 MeV. Measured neutron cross sections corresponding to the inelastic excitation of groups of levels to excitations of >2.5 MeV were consistent with non-elastic cross sections deduced from the measured neutron total and elastic-scattering cross sections and define energy-transfer mechanisms of interest in applied-neutronics calculations. ^{107}Ag is a fission product and the above model, verified in the present measurement context, provides a suitable mechanism for the provision of nuclear data for similar, but experimentally difficult, fission-product nuclides.

ACKNOWLEDGEMENTS

The authors are indebted to Dr. D. Reitmann for making available results of studies of ^{107}Ag excited structure prior to publication and for his helpful comments throughout this work. The assistance and advice of Dr. P. A. Moldauer is greatfully acknowledged, particularly in providing the model codes and instruction for their use.

REFERENCES

1. M. G. Mayer and J. Hans D. Jensen, "Elementary Theory of Nuclear Shell Structure," John Wiley and Sons, Inc., London (1955).

2. D. Reitmann, E. Barnard, D. T. L. Jones and J. G. Malan, Proc. Conf. on Nucl. Cross Sections and Technology, National Bureau of Standards Pub., NBS-SP-425, Vol. II, 879 (1975).

3. J. Rainwater, Phys. Rev., 79 432 (1951).

4. The authors are indebted to E. Kobisk et al., (Oak Ridge National Laboratory) for fabrication of the requisite silver sample.

5. D. Miller, "Fast Neutron Physics," Vol II, Eds. J. Marion and J. Fowler, Interscience Pub., N.Y. (1963).

6. A. Langsdorf, J. Monahan and W. Reardon, "Tabulation of Neutron Energies from Monoenergetic Protons on Lithium," Argonne National Laboratory Report, ANL-5219 (1954).

7. A. Smith, R. Holt and J. Whalen, "Neutron Scattering from ^{12}C in the Few MeV Region," Argonne National Laboratory Report, ANL/NDM-43 (1978).

8. S. Cierjacks, P. Forti, D. Kopsch, L. Kropp, J. Nebe and H. Unfeld, "High Resolution Total Neutron Cross Sections between 0.5-30 MeV," Karlsruhe Report, KFK-1000 (1968).

9. G. James, Proc. Sym. on Neut. Standards and Applications, National Bureau of Standards Pub., NBS-SP-493 (1977).

10. A. Smith and J. Whalen, "Comments on Energy-Averaged Neutron Total Cross Sections," Argonne National Laboratory Report, ANL/NDM-33 (1977).

11. S. A. Cox and P. R. Hanley, IEEE Trans. Nucl. Sci., NS-18 No. 3 108 (1971).

12. A. Smith, P. Guenther and R. Sjoblom, Nucl. Instr. and Methods, 140 397 (1977).

13. P. Guenther, A. Smith and J. Whalen, Phys. Rev., C12 1797 (1975).

14. J. Hopkins and G. Breit, Nucl. Data, A9 137 (1971).

15. P. T. Guenther, Univ. of Ill. Thesis, Elastic and Inelastic Neutron Scattering from and Even Isotopes of Tungsten (1977).

16. Neutron Cross Sections, 3rd Ed., Vol. II, Eds. D. Garber and R. Kinsey, Brookhaven National Laboratory Report, BNL-325 (1976).

17. Evaluated Nuclear Data File - B(ENDF/B), Version IV, National Nuclear Data Center, Brookhaven National Laboratory.

18. A. B. Smith, P. T. Guenther and J. F. Whalen, Nucl. Phys., A244 213 (1975).

19. D. Reitmann, Private Communication.

20. J. W. Meadows and D. L. Smith, "Neutrons from Proton Bombardment of Natural Lithium" Argonne National Laboratory Report, ANL-7938 (1978).

21. F. E. Berstrand and D. J. Horen, Nuclear Data Sheets for A = 107, B7 1 (1972).

22. A. Gilbert and A. G. W. Cameron, Can. Jour. Phys., 43 1446 (1965).

23. CINDA 76/77, and subsequent supplements, IAEA Press, Vienna (1976).

24. P. Hodgson, "The Optical Model of Elastic Scattering," Oxford Press, London (1963).

25. W. Hauser and H. Feshbach, Phys. Rev., 87 366 (1952).

26. P. A. Moldauer, Phys. Rev., 171 1164 (1963); and Private Communication.

27. ABAREX-1 and 2, Digital Computer Programs, P. A. Moldauer, to be published.

28. C. Engelbrecht and H. Fiedeldey, Ann. Phys., 42 262 (1967).

29. A. B. Smith, J. F. Whalen, E. Barnard, J. A. M. DeVilliers and D. Reitmann, Nucl. Sci. and Eng., 41 63 (1970).